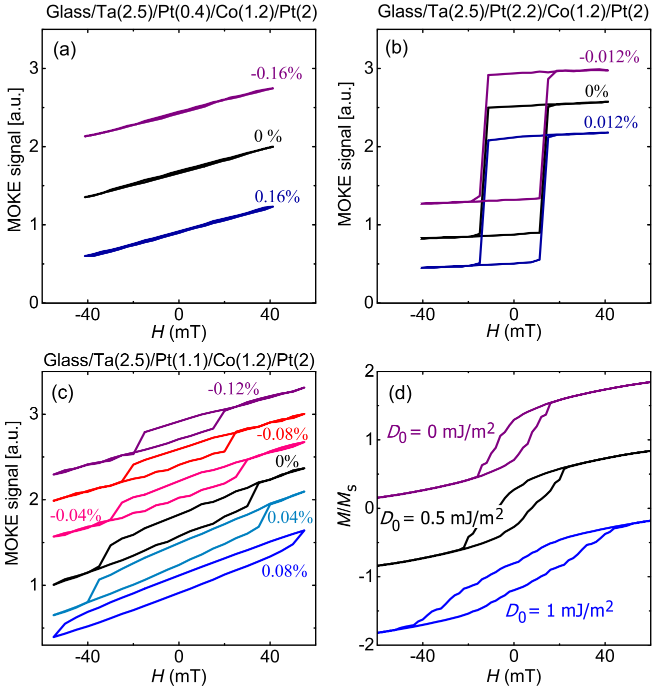

FIG. 2. Out-of-plane hysteresis loops for different strain $\varepsilon_{\rm xx}$ (shown nearby each curve) applied to the samples Glass/Ta(2)/Pt($d_{\rm Pt}$)/Co(1.2)/Pt(2). Panel (a) - $d_{\rm Pt}$ = 0.4 nm, (b) - $d_{\rm Pt}$ = 1.1 nm, (c) - $d_{\rm Pt}$ = 2.2 nm. (d) Micromagnetic simulation results for Co/Pt films. Top row is magnetization hysteresis loops for films with the different DMI: $D_0 = 0$ mJ/m^2, $D_0 = 0.5$ mJ/m^2, and $D_0 = 1$ mJ/m^2. The corresponding values of the hysteresis widths are 34, 44 and 86 mT. The loops are shifted with respect to each other for clarity.

multilayers (of order of 1 mJ/m^2). This restricts using of insulator/FM systems in skyrmionics. Voltage-induced variation of the DMI due to the charge accumulation is challenging in HM/FM multilayers since the electric field is screened in a very thin interfacial layer. In contrast, the strain-based approach proposed in the present work can be applied to metallic system giving a promising opportunity to control the skyrmions.

In the present work, a series of samples Glass/Ta(2.5 nm)/Pt($d_{\rm Pt}$)/Co(1.2 nm)/Pt(2 nm) were fabricated using DC magnetron sputtering. The thickness of the bottom Pt layer ($d_{\rm Pt}$) varies from 0.4 to 2.2 nm. Fabricating samples with different Pt thickness allows to find the one which is the most sensitive to a strain. In our samples the Co film are surrounded by two Pt layers. One can expect that DMI cancels in this case. However, well known that the nonzero DMI is observed in such symmetric Pt/Co/Pt systems [22]. This is because Pt/Co and Co/Pt interfaces actually are not identical, since the bottom Pt layer grows on the Ta buffer, while the upper Pt layer grows on Co. Moreover the DMI strongly depends on Pt thickness [23] which also makes the contributions of the upper and bottom interfaces different.

Magnetic hysteresis loops of the samples were measured at different in-plane uniaxial strain using a magneto-optical Kerr effect (MOKE) in polar geometry. A sample was placed inside the specially designed holder (see Fig. 1(a)). One edge of the sample was fixed in the holder, the opposite edge was bent by a screw inducing a uniaxial strain. The strain is elastic and does not produce a damage to the samples (see Supplementary materials). The shift of the sample free edge caused a strain of the magnetic film in the vicinity of the fixed side, where the laser beam irradiates the film. Introducing the x-axis connecting fixed and free edges (Fig. 1(a)) one can estimate the x-component of the strain as $\varepsilon_{xx} = 3d\Delta z/(2L^2)$ [24], where d and L are the thickness and length of the sample (glass plate), correspondingly, and Δz is the shift of the plate free end. The in-plane deformation was also checked using a strain gauge.

Figure 2 shows the magnetization curves of the Co/Pt samples for different $d_{\rm Pt}$. Each panel in Fig. 2 demonstrates several hysteresis loops corresponding to different strain, ε_{xx}. The panel (a) shows the case of small Pt thickness, in which the structure has an in-plane anisotropy and is not sensitive to the applied strain. The sample with the thick Pt layer (panel (b)) has a rectangular magnetization curve and no magnetostriction. The strain influences the properties of the film only when the Pt layer is close to the critical thickness at which transition between in-plane and out-of-plane anisotropy occurs. This case is shown in panel (c). The curves in this plot consist of a linear slope and a hysteresis loop. Black line in the panel represents the unstrained film. Compressive strain increases the hysteresis loop width while tensile strain reduces it. Two additional samples were also studied with the thickness of Pt layer in the range between 1.1 and 2 nm. They have a hysteresis loop similar to the sample with $d_{\rm Pt}$ = 1.1 nm. They also demonstrate the dependence of the hysteresis loop on the strain.

The DMI in the samples was studied by the Brillouin light scattering (BLS) in the Damon-Eshbach geometry [25] under application of strain in the similar way as described in the previous section (see Fig. 1(a)). A magnetic field was applied either along the deformation direction or perpendicular to it allowing us to measure the DMI constants along x (D_x) and along y (D_y) directions. Typical BLS spectrum is presented in Fig. 1(b). Solid lines show the Lorentzian fit demonstrating the shift of the Stokes and anti-Stokes peaks denoted as Δf.

Following the standard approach (see Supplementary materials) we estimated the DMI constant as [25 and 26]

$$D_i = 2M_{\rm s}\Delta f/(\pi\gamma k_i), \tag{1}$$

where $M_{\rm s}$ is the saturation magnetization, Δf is the difference between the Stokes and anti-Stokes frequencies, and k_i is the momentum along the i-direction (in our case $i = x$ or y), and γ is the gyromagnetic ratio. The value of $M_{\rm s}$ used in our estimations is $1.1 \cdot 10^6$ A/m which is typical for Co/Pt films [27 and 28].

The DMI constant along the x-direction for the three samples with the Pt thickness varying from 0.4 nm to